

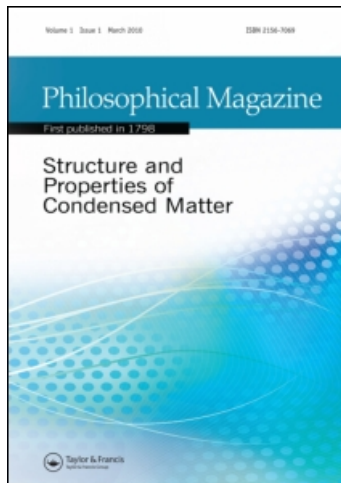
This article was downloaded by: [Widom, M.]

On: 16 May 2011

Access details: Access Details: [subscription number 937672801]

Publisher Taylor & Francis

Informa Ltd Registered in England and Wales Registered Number: 1072954 Registered office: Mortimer House, 37-41 Mortimer Street, London W1T 3JH, UK



Philosophical Magazine

Publication details, including instructions for authors and subscription information:
<http://www.informaworld.com/smpp/title~content=t713695589>

Cell-constrained melt-quench simulation of *d*-AlCoNi: Ni-rich versus Co-rich structures

M. Mihalkovič^a; M. Widom^b; C. L. Henley^c

^a Institute of Physics, Slovak Academy of Sciences, 84511 Bratislava, Slovakia ^b Department of Physics, Carnegie Mellon University, Pittsburgh, PA 15213, USA ^c Department of Physics, Cornell University, Ithaca, NY 14853-2501, USA

First published on: 15 October 2010

To cite this Article Mihalkovič, M. , Widom, M. and Henley, C. L.(2011) 'Cell-constrained melt-quench simulation of *d*-AlCoNi: Ni-rich versus Co-rich structures', *Philosophical Magazine*, 91: 19, 2557 – 2566, First published on: 15 October 2010 (iFirst)

To link to this Article: DOI: 10.1080/14786435.2010.515264

URL: <http://dx.doi.org/10.1080/14786435.2010.515264>

PLEASE SCROLL DOWN FOR ARTICLE

Full terms and conditions of use: <http://www.informaworld.com/terms-and-conditions-of-access.pdf>

This article may be used for research, teaching and private study purposes. Any substantial or systematic reproduction, re-distribution, re-selling, loan or sub-licensing, systematic supply or distribution in any form to anyone is expressly forbidden.

The publisher does not give any warranty express or implied or make any representation that the contents will be complete or accurate or up to date. The accuracy of any instructions, formulae and drug doses should be independently verified with primary sources. The publisher shall not be liable for any loss, actions, claims, proceedings, demand or costs or damages whatsoever or howsoever caused arising directly or indirectly in connection with or arising out of the use of this material.

Cell-constrained melt-quench simulation of *d*-AlCoNi: Ni-rich versus Co-rich structures

M. Mihalkovič^{a*}, M. Widom^b and C.L. Henley^c

^a*Institute of Physics, Slovak Academy of Sciences, 84511 Bratislava, Slovakia;*

^b*Department of Physics, Carnegie Mellon University, Pittsburgh PA 15213, USA;*

^c*Department of Physics, Cornell University, Clark Hall, Ithaca, NY 14853-2501, USA*

(Received 30 June 2010; final version received 9 August 2010)

Complex crystalline ground state structures may be obtained by direct (simulated) quenches from the melt for systems of up to a few hundred atoms, given the constraint of a fixed unit cell, coupled with use of (i) replica-exchange Monte Carlo, and (ii) realistic empirical interaction pair potentials. We applied this procedure to decagonal approximants of Al₇₂Co₈Ni₂₀ and Al₇₃Co₂₇, obtaining the best energies seen to date for *d*-AlCoNi models (respectively +20 meV/atom and +9 meV/atom above the tie-plane of competing phases). We elucidated the reasons why different decagonal structures are associated with the Ni-rich and Co-rich compositions. We found a cell doubling to $c = 8 \text{ \AA}$ due to layer puckering not only in the Co-rich structure, but (locally) in the nominally $c = 4 \text{ \AA}$ Ni-rich structure.

Keywords: molecular dynamics; effective Hamiltonian; Al-TM; *ab initio* energies

1. Introduction

This work is part of an effort to understand the structure and stability of decagonal *d*-AlNiCo, the highest quality decagonal quasicrystal. Due to the complexity of the structure, and averaging-over-disorder effects, even good diffraction datasets [1,2] cannot reliably provide the precise structure – not well enough to predict the well-known fact that *d*-AlCoNi is thermodynamically stable with respect to the competing crystal phases owing to their excess energy relative to competing crystals.

Previous simulation studies derived low-energy structural models on the Ni-rich [3,4] and Co-rich [5–7] compositions, or on the whole range [8] by first Monte Carlo annealing a lattice-gas on discrete sites (augmented by tile-reshuffling moves). The prerequisites for that method were (i) realistic pair potentials; (ii) ‘minimal experimental input’ in the form of the layer spacing and quasilattice constant (i.e. tile size); and (iii) most importantly the fact of layering, and the assumption of near-ideal candidate atomic positions.

In agreement with experiment, these studies arrived at similar but distinct structure types in the Ni-rich and Co-rich cases, which we will call ‘Ni type’ and

*Corresponding author. Email: mihalkovic@savba.sk

‘Co type’ for short. The Ni-type structure is based on hexagon/boat/star (HBS) tiles (at a hierarchy of length scales [3]) and, according to experiment, has a stacking period of 4 Å along the 10-fold axis; the HBS tiles group into (possibly overlapping) decagonal clusters with diameter 20 Å, having central motifs with (only) mirror symmetry, appearing as triangles of TM atoms in high-resolution electron microscope images.

The Co-type structure, although it contains HBS tiles also, is dominated by 20 Å non-overlapping decagon clusters which we shall call ‘pentagonal decagons’ (PD). Other prominent features are clusters similar to pentagonal bipyramids (PB), centered on the perimeter of the 20 Å decagons and forming columns in which some Al atoms pucker out of the layers in alternate directions, causing a cell doubling to $c = 8 \text{ Å}$ in the stacking direction.

We believe the key reason for the excess energy is the displacement of certain Al atoms out of the main atom layers, called ‘puckering’. This is explained in terms of ‘channels’ [4–6]: linear potential wells for Al atoms that are aligned transverse to the atom layers, located between two columns of TM atoms. The Al atoms, when packed tightly into the channels, must be spaced $\sim 2.6 \text{ Å}$, i.e. 1.3 layers apart, so that three Al atoms fit in four layers. Hence, locally in any channel, the stacking period gets doubled from two to four layers; only one of the three atoms aligns with a layer, which becomes the local mirror plane of that channel. Puckerings occur, as a form of *local* order, even in alloys whose *average* structure is just two layers. Consequently, *diffuse* scattering [9–12] is observed corresponding to the four-layer local order, and this diffuse scattering shows elaborate modulations within the 10-fold layer due to correlations between the phases of puckering in nearby ‘channels’. Thus a successful understanding of those correlations will also give the first theory for this diffuse scattering.

Structure models without puckering at all are many tens of meV/atom too high in energy. Allowing puckering locally can capture half of this energy but is still not sufficient to obtain the lowest energies. For that, we must incorporate the correct *correlations* between the signs of puckering of Al atoms in nearby channels, since these atoms interact strongly. (A weakness of our past approach [3,5] is that the discrete site list used initially does not incorporate puckering displacements.) No simple recipe is known for the global puckering pattern. Note that *d*-AlNiCo has a well-known zoo of structural modifications [20] which depend on tiny differences in composition, and (we suspect) go with different puckering patterns.

2. Cell-constrained melt-quench method

One of the most challenging tasks of contemporary material science, and the basic question in our studies of quasicrystal structures is: given a composition, what is the optimum structure? A general method was put forward using ideas of genetic algorithms and including variation of the cell, as implemented in the program USPEX [13], but apparently this cannot yet handle systems with complex structure.

We have developed an approach we call ‘cell-constrained melt-quench’ which is surprisingly successful at predicting *low-temperature* structures of complex alloys with hundred(s) of atoms per cell. This simply means cooling the system under

brute-force molecular dynamics using periodic BCs in a small cell, while fixing the composition, atomic density, and the unit cell of the system to the experimentally known values. Quite often those are available experimentally from electron diffraction or powder diffraction, when single-crystal structure refinement is impossible. The ‘cell constraint’ seems to limit the ensemble of possible states so we can shepherd the system to the global energy minimum.

One’s expectation is that, in a multi-species system described by oscillating interatomic potentials [3], such a quench should get caught in a glassy or highly defective metastable state rather than the true energy minimum. But we found it was sufficient to apply the trick of ‘replica exchange’ (‘parallel tempering’) [14–16], wherein a set of simulations is run, each at a different temperature, and the entire configuration may be exchanged between temperatures according to a Metropolis step. (Note that within each loop, we perform not only MD but also MC steps that swap the species of two atoms.)

Of course, it is also crucial to have realistic pair potentials. These may be constructed systematically (as with Moriarty’s GPT potentials [27,28] which we used in this project). Alternatively, for Al-transition metal (Al-TM) and many other alloys, one does just as well with empirical potentials including Friedel oscillations that can quickly be fitted to an appropriate database of *ab initio* energies and forces [18]. Empirical potentials (specified by a few parameters) may be fitted to data sets of *ab initio* forces and energies.

The general philosophy of this method – taking advantage of lattice and composition information to moderately constrain the simulation – also inspired our earlier work based on quasi-lattice-gases [3,7]. In the present approach, we need fewer assumptions, and the method directly finds good answers for the (intricate) patterns of atoms deviating out of the layers, which turns out to be the crucial unresolved aspect of the structure model.

The cell-constrained method has been successful for a variety of intermetallics.¹ For example, in the *i*-CaCd family of structures, this method successfully gave the starting point for a Rietveld refinement of the ‘2/1-1/0-1/0’ AlCuSc approximant [17].

3. Set-up for Al–Co–Ni melt-quench study

Our simulations used the realistic GPT pair potentials [27,28] as we used before [3,7,5]. The cell sizes for decagonal approximants are all based on tilings with lattice constants $a_q = 2.44 \text{ \AA}$ in-plane, and $c = 4.08 \text{ \AA}$ for the minimum stacking period.

The melt-quench (MQ) simulation was set up with 20 annealing temperatures distributed between 1000 and 2500 K. One tempering cycle consisted of 1000 MD steps with time increment $\Delta T = 0.2 \text{ fs}$, followed by a Metropolis Monte Carlo (MC) loop of 7800 attempted species swaps (the acceptance rate was 0.03–0.05). Typically, for a system of this size the simulation needs ~ 100 steps until first metastable low-energy configurations appear. Occasionally, we take the current lowest-temperature sample and quench it to monitor the energy of the underlying zero-temperature state.

To validate our method, we first verified that cell-constrained quenching with GPT potentials [27,28] reproduced *all* Al-rich binary structures in the Al–Co and Al–Ni systems, as well as the ternary phase *X*-AlCoNi.

With Al–Ni, we verified that $12\text{Al} + 4\text{Ni}$ in the orthorhombic unit cell of Al_3Ni (16 atoms $6.6 \times 7.4 \times 4.8 \text{ \AA}$) easily reproduced that structure after just 10 loops. On the Co-rich side, the essential test was the orthorhombic $\text{Al}_{13}\text{Co}_4$ phase; the monoclinic (fully occupied) version $m\text{-Al}_{13}\text{Co}_4$ with 51 atoms per primitive cell was exactly recovered after 119 loops. We also reproduced Al_9Co_2 .

Finally, we checked the ternary $\text{X}(\text{AlCoNi})$ phase [24] which has ratio 18:5:3 Al:Co:Ni in a monoclinic unit cell: the structure was observed after 71 loops. The longest of the test simulations ($m\text{-Al}_{13}\text{Co}_4$) needed just a few minutes on a standard quad-core PC, demonstrating the efficiency of the method for system sizes up to ~ 50 atoms per simulation box.

First we show the results of simulations in a larger unit cell we call the ‘2B + H cell’ since it accommodates two boat tiles and one hexagon tile of edge 6.5 \AA per primitive cell; the cell is centered orthorhombic with cell parameters (in a monoclinic setting) $a = b = 19.78 \text{ \AA}$, $\gamma = 108^\circ$, and $c = 8.06 \text{ \AA}$. With composition $\text{Al}_{0.75}\text{Co}_{0.25}$, we obtain a decagonal approximant (Figure 1a). On the other hand, using our standard Ni-rich composition $\text{Al}_{148}\text{Co}_{16}\text{Ni}_{41}$ in this cell, we obtain the B2 structure (Figure 1b).

The chief technical hindrance to obtaining decagonal approximants is competition from the B2 phase (Figure 1b), which has ideal composition $\text{Al}(\text{Co}, \text{Ni})$ in which Co and Ni substitute each other. Since B2 has a small unit cell, it fits with moderate distortion into almost every one of our simulation cells. B2 is a thermodynamically stable phase *at high temperatures*, and is probably more accessible than the desired phases. We ascribe both properties to the very large

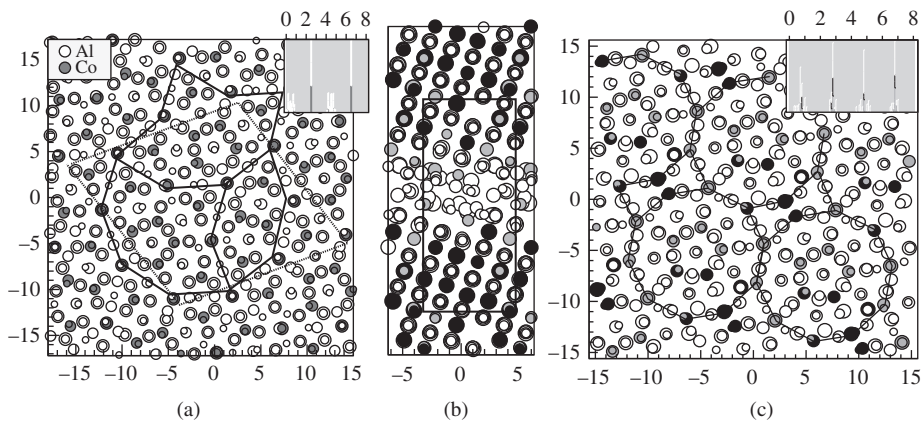


Figure 1. (a) Various outcomes of constrained-cell melt-quench simulation. The ‘2B + H’ unit cell is tractable on the Co-rich side, here $\text{Al}_{158}\text{Co}_{52}$. Here and in Figure 2, the view is along the short (c) axis; atoms are marked by circles, with larger sizes denoting larger z coordinate. Lines show bonds between atoms in different layers: heavy and light for TM–TM and Al–Al, with projected lengths $4.1 \pm 0.3 \text{ \AA}$ and 2.6 \AA , respectively. (b) A B2-like structure found in the same cell for Ni-rich composition $\text{Al}_{148}\text{Co}_{16}\text{Ni}_{41}$ viewed along the $(1, 1, 0)$ direction (c axis is horizontal). (c) Co-rich ‘Co-type’ MQ structure $\text{Al}_{58}\text{Co}_{14}\text{Ni}_9$, ‘boat’ cell. Composition similar to W-phase [25].

configurational entropy of Al/vacancy/(Co, Ni) on the sites of B2 structure, as necessitated by our Al-rich compositions.

Due to their unrealistically deep Al–TM nearest-neighbor wells, the GPT pair potentials exaggerate the stability of B2. Still, it is known experimentally that B2-Al(Co, Ni) (with TM site disorder) does coexist with decagonal phases in AlCoNi samples carefully annealed at high T [19].

4. Results

To avoid formation of the spurious B2 phase, we adopted a simulation cell smaller in linear dimensions by a factor $\tau \equiv (1 + \sqrt{5})/2 \approx 1.618$ that we believe matches the B2 phase poorly. It is centered orthorhombic with lattice constant $a = b = 12.3 \text{ \AA}$, $\gamma = 108^\circ$ in monoclinic setting, and $c = 8.20 \text{ \AA}$ (so the layer spacing is 2.05 \AA). Each primitive cell accommodates one τ^2 -inflated boat tile of edge 6.4 \AA . (In the orthorhombic setting, the cell is $a = 14.36 \text{ \AA}$, $b = 19.69 \text{ \AA}$ and $c = 8.16 \text{ \AA}$.) Also, the approximate composition of the Ni-rich decagonal is reported to be $\text{Al}_{72}\text{Co}_8\text{Ni}_{20}$. So we studied various cell contents, most importantly $\text{Al}_{56}\text{Co}_6\text{Ni}_{16}$ at the Ni-rich end (with variations having 57 Al and/or 15 Ni), and $\text{Al}_{58}\text{Co}_{14}\text{Ni}_9$ at the Co-rich end.

Atomic density is a key parameter; experimentally reported values in d -AlCoNi vary from $0.066 \text{ atoms/\AA}^3$ according to [23] up to $0.070 \text{ atoms/\AA}^3$ (see the references in [22]). Our runs explored this whole range which corresponds to 77–80 atoms per primitive cell. We call a structure ‘high density’ when it has 58 or 57 Al atoms in the ‘boat’ cell (see Figure 2).

As expected, we could obtain both Ni-type and Co-type decagonal structures in different compositions. What was unclear *a priori* was (i) are these two discrete possibilities, or is there a gradual continuum of types interpolating between them?; (ii) What determines which of the types is seen?

For our chosen Ni-rich composition, depending on whether we used a low or high atom density, we obtained either the Ni-type structure or the Co-type structure,

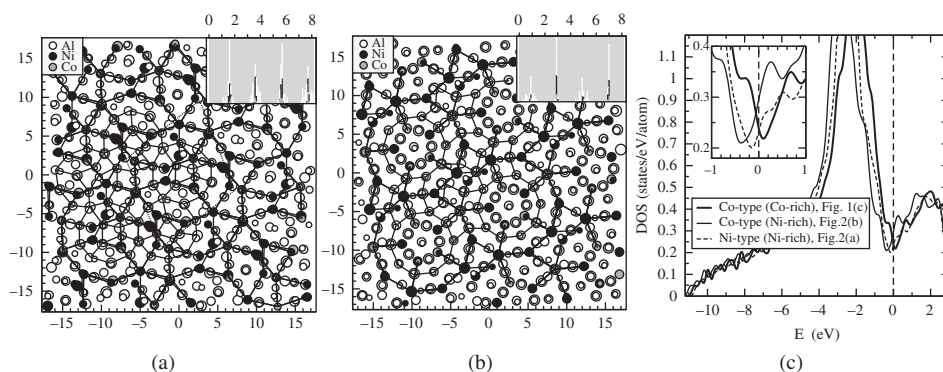


Figure 2. (a, b) Ni-type or Co-type structures emerge in the ‘boat’ cell, for (respectively) lower density ($\text{Al}_{56}\text{Co}_6\text{Ni}_{16}$) or higher density ($\text{Al}_{58}\text{Co}_{14}\text{Ni}_9$). (c) Electronic density of states $e(\text{DOS})$ for three cases: Co-type Co-rich ($\text{Al}_{58}\text{Co}_{14}\text{Ni}_9$ in Figure 1c), Co-type Ni-rich (Figure 2b), and Ni-type Ni-rich (Figure 2a).

corresponding to the respective low and high densities of these phases. (Specifically, the Co-type structure occurred with 58 or 57 Al atoms/cell.) By contrast, for Al–Co at any density (and composition), the optimum structure (as found by the simulation) is always Co-type. If a lower density is used, Al–Co will incorporate vacancies, rather than switch to the lower-density Ni-type structure.

We find that only the discrete Ni-type and Co-type optimal low-temperature structures are found. A prominent motif found in both structure types is the ‘D-ring’ of diameter 12 \AA , consisting of 10 TM atoms alternating from one layer to the other, spaced by 4.0 \AA in-layer, or actually 4.5 \AA between atoms (which is very favorable for the TM-TM potentials). Remarkably, D-rings have even been observed superimposed on the disordered B2 type structure. It is likely that the D-rings form at temperatures where the Al atoms are still relatively disordered (we know from other simulation studies that TM-TM order precedes Al order [32]).

The Co-type structure seemed essentially unique, since (with long annealing times) several independent quench runs arrived at identical states (apart from some variation between Ni and Co on TM sites). On the other hand, annealing the Ni-type structure gave a different HBS tiling every time. What was robust in the Ni-type structure was the (often overlapping) D-rings.

5. Puckering

We find not only Co-rich but Ni-rich structures are *locally* 8 \AA periodic. A convenient summary of the puckering behavior is seen in the distribution function of the atoms’ z coordinates, as shown by insets in each figure.

The Co-type structures all contain four layers of thickness 2 \AA : two perfectly flat (mirror) layers alternating with two puckered layers. The reasons for this kind of ordering were laid out in Ref. [6]; a long range order can propagate because there is a well connected network of channels across the system. The $\text{Al}_{58}\text{Ni}_{22}$ sample (in a Co-type structure) shows the same puckering behavior as the Co-rich sample.

By contrast, in the Ni-type structures found at lower atomic densities all four layers have some puckered atoms: Figure 2a, inset. That means each layer has a mixed nature: for some ‘channels’ it is a (local) mirror layer, but for others it is a (local) puckered layer. Presumably, the Ni-type system has *statistical* 4 \AA period despite its *local* 8 \AA ordering, because the puckered motifs are rarer and less correlated.

In both types of decagonal structures, one finds certain columns of TM atoms surrounded by five neighboring TM columns 4 \AA away. In the Ni-type structure, this happens at the center of every star tile of the small HBS tiling in Figure 2a. In the Co-rich type structure [6], it occurs on every other vertex of the D-ring which bounds the 12 \AA decagon (Figure 2b). Such columns are surrounded by five ‘channels’, which have strongly correlated puckering patterns due to steric constraints. In Ref. [6] we identified a characteristic motif of such ‘puckering centers’, called the ‘crooked cross’, and it is in fact visible in every puckering center in Figures 1a and 2a and b. This consists (in projection) of a pair of puckered Al atoms at the same z and on opposite sides of the central TM; a second such pair lies at a different z and (in projection) roughly at right angles to the first. (These atoms stand out in the

figures because they are the only ones whose projections do not lie on ideal quasilattice sites.)

Finally, the $\text{Al}_{0.75}\text{Co}_{0.25}$ structure of Figure 1a has the same puckering pattern as in the well-known $\text{Al}_{13}\text{Co}_4$ structure. Some puckered atoms are an intrinsic part of the ‘pentagonal bipyramid’ motif [21,22]; on top of the same cluster there is an atom pair, as in a ‘crooked cross’, but the other arm of the cross is missing, because an Al atom appears right on the local five-fold axis at the same z (a mirror-layer) that the second two atoms would have been (and excludes them sterically).

To demonstrate how essential the local puckering is, we ran the same Ni-rich composition while replacing the 8 \AA cell constraint by 4 \AA . The resulting structure contains *no* clearly pentagonal motifs; instead, it somewhat resembles the 4 \AA periodic phase $X(\text{AlCoNi})$ [24]. Although its pair-potential energy is practically degenerate with the (8 \AA) decagonal’s, we never observed the 4 \AA phase in the 8 \AA box: presumably its entropy is too small.

6. *Ab initio* calculations of phase stability

Having obtained structures from cell-constrained simulations with pair potentials, we check their (relaxed) energy *a posteriori* using the *ab initio* program VASP [29–31]. Our criterion for stability is a zero-temperature energy of at most 10 meV/atom above the tie-plane of other phases. Note that a small excess energy is often compensated in quasicrystals *and* approximants by a higher vibrational entropy not found in other alloy structures, meaning the quasicrystal, or approximant, is stable as a high-temperature phase.

For the Al–Co alloy system [22] and the Al–Ni binary and also the Al–Co–Ni ternary system, we evaluated the total energies of all experimentally stable Al-rich phases (except $\epsilon\text{-Al}_3\text{Co}$, which at 342 atoms/cell is too large to handle). We constructed the convex hull of coexistence tie-planes on the plot of energy as a function of composition; our energies are quoted relative to the convex hull defined by Al_3Ni , Al_3Ni_2 , Al_9Co_2 , and Al_5Co_2 .

We pause for a moment to sketch the ‘energy landscape’ of these competing phases. $X\text{-Al}_9\text{Co}_2\text{Ni}_2$ had energy 8.5 \AA above the tie-line [24] ($+6.1\text{ meV}$ for composition $\text{Al}_9\text{Co}_{2.5}\text{Ni}_{1.5}$), and $W\text{-AlCoNi}$ had energy $+12.0\text{ meV}$ [26]. Al_9Co_2 remains stable in a ternary composition (replacing $\text{Co} \rightarrow \text{Ni}$) up to 9% Ni. Note that [22] $\text{Al}_{13}\text{Co}_4$ is a *high-temperature* phase, stabilized by vibrational and vacancy/substitutional entropy; at full occupancy, it is unstable by 10 meV/atom .

The decagonal approximant structures we obtained had the best energies seen to date for any $d\text{-AlCoNi}$ models with the Ni-rich and Co-rich composition, respectively $+20\text{ meV/atom}$ (Figure 2a) and $+19\text{ meV/atom}$ (Figure 1c) above the convex hull of low-temperature competing phases. It turns out that Al–Co has quite good energies in typical Al–Ni structures (e.g. nearly stable in the Al_3Ni structure), but not vice versa: structures favorable for Al–Co, e.g. ($\text{Al}_{13}\text{Co}_4$ or Al_5Co_2) are *highly unfavorable* in the Al–Ni system. The well-ordered Co-type structures are unstable with Ni-rich compositions, by $+53\text{ meV/atom}$ ($\text{Al}_{58}\text{Co}_6\text{Ni}_{16}$). For lower densities, optimal structures were always Ni-type: unstable by $+36\text{ meV/atom}$ ($\text{Al}_{57}\text{Co}_6\text{Ni}_{16}$), optimally $+20\text{ meV/atom}$ ($\text{Al}_{56}\text{Co}_6\text{Ni}_{16}$), and by $+24\text{ meV/atom}$ at even lower density

cell content ($\text{Al}_{56}\text{Co}_6\text{Ni}_{15}$). For Al–Co the *best* decagonal-like structure is always Co-type; in particular, $\text{Al}_{0.75}\text{Co}_{0.25}$ in Figure 1a is just 7.5 meV/atom unstable against decomposition to Al_9Co_2 and Al_3Co .

We now come to the point why (in reality) the (nearly) stable decagonal-type structures are Ni-type for Ni-rich compositions and Co-type for Co-rich compositions. For Co fraction above $\sim 25\%$ the Al–Co binary is destabilized by competition with Al_5Co_2 : nothing breaks structurally in the decagonal, but the tie-line is simply pulled down by the very good Al_5Co_2 energy. Conversely, in the Al–Ni system, decagonals with low Ni content are destabilized by competition with Al_3Ni . From this viewpoint, the fact that Al–Ni phases are low-density and Al–Co phases are high-density is an accident of the different landscape of competing non-quasicrystal phases.

A different viewpoint explains the difference within the decagonal phase itself. When we examine the electronic density of states (Figure 2c) we see a prominent pseudogap as in most Al–TM quasicrystal-like phases. The optimum stability occurs when the Fermi level coincides with the pseudogap. But since Ni has a different (effective) valence than Co, we need different density and compositions in order to achieve this matching of the Fermi energy. Clearly, the ‘high-density’ Co-type Ni-rich structure of Figure 2b is disfavored by this effect – see the thin line in Figure 2c.

7. Discussion

In summary, we obtained excellent structural energies from direct quenching molecular dynamics with pair potentials, when constrained by cell parameters and aided by realistic potentials as well as replica-exchange and other Monte Carlo steps. The size limit on our unit cell was not from the computer time needed to anneal it, but rather from the need to ensure that unwanted high-temperature phases are mismatched with the lattice parameters. We found there are two discrete structure types, and explained (Section 6) why one goes with Ni-rich compositions and the other with Co-rich compositions. Ultimately, we believe the physical parameter controlling the phase is electron density (which tracks atom density): higher or lower electron densities are optimal for Co-rich or Ni-rich compositions, respectively.

There is no hope to realistically model *any* decagonal without (at least local) 8 \AA period due to ‘puckering’ of Al atoms out of their layers, as emphasized by the failure to obtain a decagonal in a 4 \AA cell. Note that the best energy for Ni-rich *d*-AlCoNi found here is comparable to the best energy found by hand-built variations and/or MD-relaxations applied to the tile-decoration model approach.² Thus, each structure includes some feature that the other one lacks. The cell-constrained quench finds the large-scale feature of the D-ring, as well as local puckerings, but probably does not find the absolute best global *correlations* of the puckerings. The decoration variations are based on a hierarchical pattern of tilings [3] with edges $\sim 2.5 \text{ \AA}$, $\sim 4.0 \text{ \AA}$, and $\sim 6.5 \text{ \AA}$, which may be superior to the quench results (which have well-defined TM positions but some Al variability); furthermore, due to a more systematic testing of puckering patterns, they may have achieved better puckering correlations.

The cell-constrained quench, thus, may ultimately not be a direct shortcut to good structures. Rather, it might replace lattice-gas Monte Carlo as a better method to use in the early stages of our recipe [3,5], where one is discovering basic decoration rules which permit further simulations at larger length scales. It will be interesting to see if decorations which ensure a high density of D-rings can reach energies as low as the melt-quench structures.

Acknowledgements

This work was supported by US Department of Energy grant DE-FG02-89ER-45405 (CLH) and by Slovak VEGA 2/0157/08. CLH acknowledges a travel fellowship from the Slovak Academic Information Agency (2010).

Notes

1. M. Mihalkovič and C.L. Henley, unpublished work.
2. M. Mihalkovič and M. Widom, unpublished work.

References

- [1] A. Cervellino, T. Haibach and W. Steurer, *Acta Crystallogr. B* 58 (2002) p.8.
- [2] H. Takakura, A. Yamamoto and A.P. Tsai, *Acta Crystallogr. A* 57 (2001) p.576.
- [3] M. Mihalkovič, I. Al-Lehyani, E. Cockayne, C.L. Henley, N. Moghadam, J.A. Moriarty, Y. Wang and M. Widom, *Phys. Rev. B* 65 (2002) p.104205.
- [4] C.L. Henley, M. Mihalkovič and M. Widom, *J. Alloys. Comp.* 342 (2002) p.221.
- [5] N. Gu, M. Mihalkovič and C.L. Henley, *Phil. Mag. Lett.* 87 (2007) p.923.
- [6] N. Gu, M. Mihalkovič and C.L. Henley (arxiv.org/abs/cond-mat/0602095).
- [7] N. Gu, C.L. Henley and M. Mihalkovič, *Phil. Mag.* 86 (2006) p.593.
- [8] S. Hiramatsu and Y. Ishii, *J. Phys. Soc. Jpn.* 75 (2006) p.054602.
- [9] F. Frey and W. Steurer, *J. Non-Cryst. Solids* 153 (1993) p.600.
- [10] F. Frey, E. Weidner, K. Hradil, M. De Boissieu, R. Currat, K. Shibata, A.P. Tsai and T.J. Sato, *Phil. Mag. A* 80 (2000) p.2375.
- [11] F. Frey and E. Weidner, *Z. Kristallogr.* 218 (2003) p.160.
- [12] M. Kobas, T. Weber and W. Steurer, *Phys. Rev. B* 71 (2005) p.224205.
- [13] A.R. Oganov and C.R. Glass, *J. Chem. Phys.* 124 (2006) p.244704.
- [14] R.H. Swendsen and J.S. Wang, *Phys. Rev. Lett.* 57 (1986) p.2607.
- [15] M.E.J. Newman and G.T. Barkema, *Monte Carlo Methods in Statistical Physics*, Oxford University Press, Oxford, 1999.
- [16] E. Lyman, F.M. Ytreberg and D.M. Zuckerman, *Phys. Rev. Lett.* 96 (2005) p.028105.
- [17] T. Ishimasa, A. Hirao, T. Honma and M. Mihalkovič, *Phil. Mag.* 91 (2011) p.2594.
- [18] M. Mihalkovič, C.L. Henley, M. Widom and P. Ganesh, *Empirical oscillating potentials for alloys from ab initio fits* (arxiv.org/abs/0802.2926).
- [19] B. Grushko, D. Holland-Moritz, R. Wittmann and G. Wilde, *J. Alloys Comp.* 280 (1998) p.215.
- [20] S. Ritsch, C. Beeli, H.U. Nissen, T. Gödecke, M. Scheffer and R. Lück, *Phil. Mag. Lett.* 78 (1998) p.67.
- [21] C.L. Henley, *J. Non-Cryst. Solids* 153&154 (1993) p.172.
- [22] M. Mihalkovic and M. Widom, *Phys. Rev. B* 75 (2007) p.014207.

- [23] P.J. Steinhardt, H.C. Jeong, K. Saitoh, M. Tanaka, E. Abe and A.P. Tsai, *Nature* 396 (1998) p.55.
- [24] S. Katrych, M. Mihalkovič, V. Gramlich, M. Widom and W. Steurer, *Phil. Mag.* 86 (2006) p.451.
- [25] K. Sugiyama, S. Nishimura and K. Hiraga, *J. Alloys Comp.* 342 (2002) p.65.
- [26] M. Mihalkovič and M. Widom, *Phil. Mag.* 86 (2006) p.557.
- [27] J.A. Moriarty and M. Widom, *Phys. Rev. B* 56 (1997) p.7905.
- [28] M. Widom, I. Al-Lehyani and J.A. Moriarty, *Phys. Rev. B* 62 (2000) p.3648.
- [29] G. Kresse and J. Hafner, *Phys. Rev. B* 47 (1993) p.R558.
- [30] G. Kresse and J. Fürthmüller, *Phys. Rev. B* 54 (1996) p.11169.
- [31] G. Kresse and D. Joubert, *Phys. Rev. B* 59 (1999) p.1758.
- [32] S. Lim, M. Mihalkovič and C.L. Henley, *Phil. Mag.* 88 (2008) p.1977.